Controlling the Inhomogeneity of Solid Catalysts at the Mesoscopic Scale

Hua Huang[1], Takahiro Wada[1,2] Hiroko Ariga[1], Satoru Takakusagi[1], Kiyotaka Asakura[1,*] and Yasuhiro Iwasawa[3]

1 Institute for Catalysis, Hokkaido University, Kita 21-10, Kita-ku, Sapporo 001-0021, Japan

2 Graduate School of Medical and Dental Sciences, Tokyo Medical and Dental University, Tokyo 113-8549, Japan

3 Innovation Research Center for Fuel Cells, Graduate School of Informatics and Engineering, The University of Electro-Communications, Chofu, Tokyo 182-8585

Abstract

High-performance catalysts are often composed of two or more active phases, which are believed to interact with each other at the mesoscopic scale structure. Unlike conventional powder catalysts flat surfaces is advantageous in that its surface structure can be precisely designed. We prepared precisely designed $Sb_2O_4/VSbO_4/Si$ catalysts containing Sb_2O_4 ribbons with finely controlled width and separation by electron lithography. We demonstrated that the acrolein generation rate on the catalysts was related to the width and separation of the Sb_2O_4 ribbons. This work shows the possibility to regulate catalyses by inhomogeneity of the surface structure at the mesoscopic level.

Introduction

Zewail has developed ultrafast electron microscopy to monitor the inhomogeneity in the chemical reactions occurring on catalyst surfaces and biological systems [1]. The next step is using this information to determine how to control the inhomogeneity of catalyst surfaces and chemical reactions. Physical control of surface reactions has been achieved using a laser spot that manipulates the chemical reaction on the mesoscopic scale [2]. Selective reactions can be induced by vibrational activation using resonance FEL-IR(Free electron laser-infrad) light [3,4]. Another method of physical control of nanostructures is to use lithography. Lithography fabricates microdevices such as LSI(large-scale integrated circuits), sensors, and MEMS/NEMS(micro/nanoelectromechanical systems). The size of each device element is also on the same scale as the inhomogeneity of catalyst surfaces and chemical reactions. However, lithography can only be applied to flat surfaces such as single crystals; it cannot be used for conventional powder samples. Metal catalysts with well-defined sizes have been fabricated by lithography to reveal the particle size effect of supported metal catalysts [5 -12].

Mixed oxides with two or more different phases usually show improved reaction performance compared with that displayed by catalysts composed of a single phase [13,14]. Wachs summarized several concepts to explain the higher performance of mixed oxides compared with that of their individual components [14]. One possible mechanism is based on the so-called “remote control mechanism” proposed by Delmon [15]; this mechanism assumes that the diffusion of lattice oxygen

occurs from one phase to the other like a phase transfer catalyst [16]. Ternary oxides that show the remote control mechanism are Sn-Sb-O, Bi-Mo-O, and V-Sb-O; these oxides consist of both oxygen donor and oxygen acceptor phases [17-21]. In the remote control mechanism, lattice oxygen generated on the oxygen donor phase is transferred to the oxygen acceptor to compensate for the oxygen consumed during the oxidation reaction at the acceptor phase. According to the remote control mechanism, the oxygen diffusion distance, ranging from a few tens of nanometers to a few tens of micrometers, is an important factor for determining the interaction between the phases. The idea of catalysis control by mass transfer was first reported in the late 1950s by Weisz and Swegler [22,23]. According to this idea, the location, separation, and size of each phase on the mesoscopic (nanometer–micrometer) scale should enable us to control catalytic performance.

In this study, we prepare precisely designed α-Sb_2O_4/$VSbO_4$/Si catalysts consisting of Sb_2O_4 microribbons with controlled width and separation by electron lithography, as shown in Fig. S1. We demonstrate that it is possible to regulate the surface reaction by artificially controlling the inhomogeneity of the surface structure on the mesoscopic scale.

Experimental

We prepared well-defined inhomogeneous α-Sb_2O_4/$VSbO_4$/Si catalysts with controlled width and separation by electron lithography on Si(100) covered with native SiO_2 (100 nm thick) [11,24]. The Sb_2O_4/$VSbO_4$ thin films were fabricated on Si substrates as shown in Fig. S1. Details of preparation procedures were described in supporting information.

Characterization has been done by XRD(RIGAKU RINT2500H using a Cu K_α line), XPS(Al Kα Kratos XSAM800) and SEM(Hitacchi S-800). Surface morphology was studied by AFM(Seiko Instrument, SPA500)

For comparison, a reference $VSbO_4$/Si catalyst was also synthesized by a sol-gel method along with spin coating [11]. Catalytic activities of the samples were tested using the selective oxidation of propene to acrolein ($C_3H_6+O_2 \rightarrow C_3H_4O+H_2O$) in a home-made batch reactor (Fig. S3).

The products were sampled and detected by a quadrupole mass spectrometer. The data were normalized under a constant Ar pressure. The acrolein generation rate was calculated by the initial rate method and then divided by the total area of $VSbO_4$ domains.

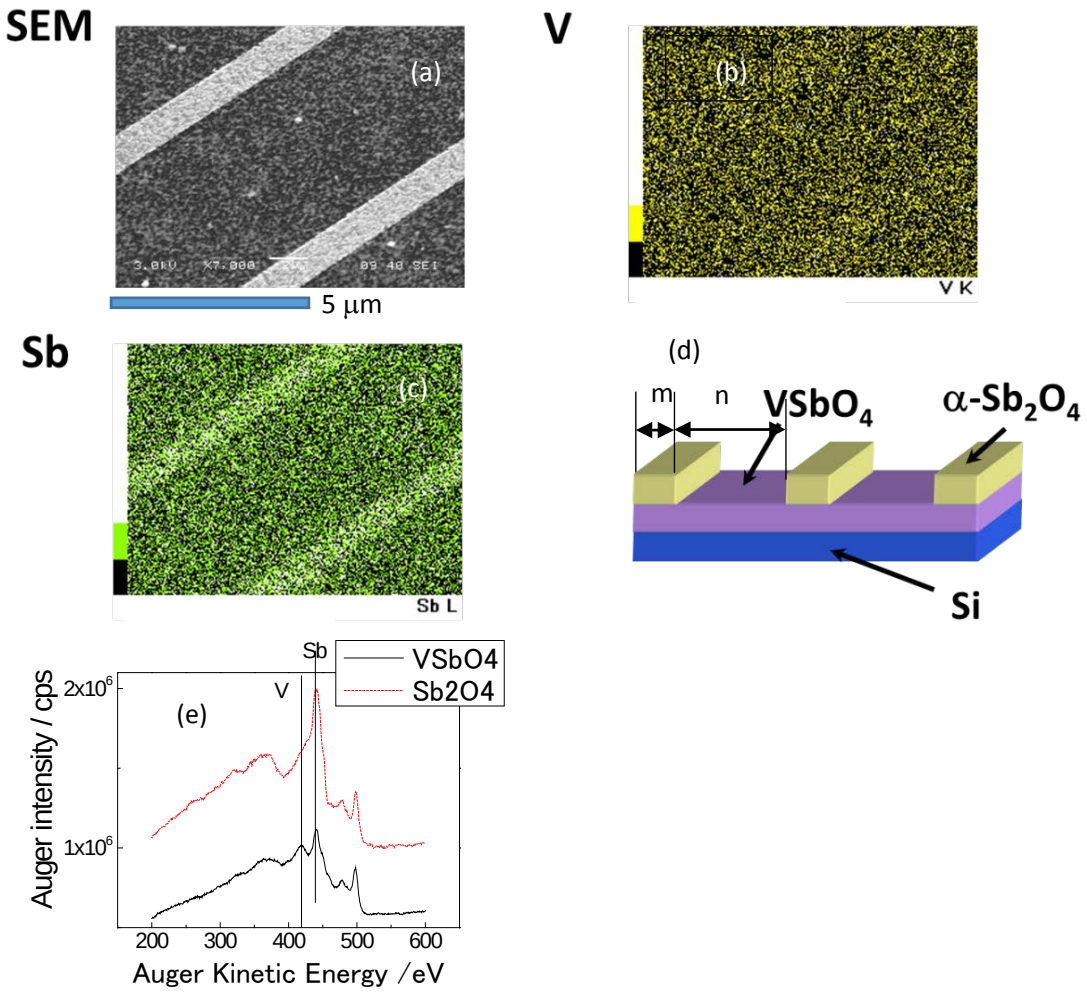

Figure 1 SEM, EDX images and spot auger spectraof the- α-Sb_2O_4/$VSbO_4$ thin film L100S400. (a) Secondary electron image, and (b) V Kα, and (c) Sb Lα fluorescence images. (d) Schematic of the sample structure.(e) spot Auger spectra of $VSbO_4$(black solid line) region and α-Sb_2O_4 region(red dotted line).

Results and discussion

Fig. 1 shows scanning electron microscopy (SEM) and its energy-dispersive X-ray spectroscopy (EDX) images of an α-Sb_2O_4/$VSbO_4$ thin film along with a schematic of the film structure(d). The samples are denoted as L(100 × *m*) S(100 × *n*) with a ribbon width of *m* μm and separation of *n* μm. Thus, L100S400 indicates that the sample contained ribbons that were 1 μm wide with a separation of 4 μm. The EDX image of V had no contrast (Fig. 1(b)) because the whole Si surface was covered

with $VSbO_4$, while α-Sb_2O_4 ribbons displayed a stronger Sb signal than the rest of the sample (Fig. 1(c)). Fig. S2 depicts the optical microscopy, laser scanning confocal microscopy (LSCM), and X-ray diffraction (XRD) results obtained for L100S400. Optical microscopy demonstrated that L100S400 contained structures that were present over a wide range of the sample. LSCM indicated that the final thickness of the α-Sb_2O_4 ribbon was 140 nm, as shown in Fig. S2(b). The catalyst has a square shape with a side length of 0.6 cm. In the latter stage this side length is denoted as *CL*. The total surface area of the catalyst was 0.36 cm^2. Since the *m:n* was constant, total area of $VSbO_4$ was constant for all α-Sb_2O_4/$VSbO_4$/Si catalysts. XRD revealed the presence of α-Sb_2O_4 and $VSbO_4$ phases (Fig. S2(c)). Figure 1(e) shows the spot Auger spectra both in $VSbO_4$ and α-Sb_2O_4 regions. Sb peaks appeared in both regions but V was found only on the VSbO4, indicating that the little diffusion of V to the Sb_2O_4 region.

Fig. S4(a) shows the initial rate for acrolein generation of the L100S400 catalyst as a function of propene partial pressure (0.1–0.8 Pa) at 523 K. The acrolein generation rate was essentially unaffected by the partial pressure of propene. Similary the rate remained nearly unchanged over the O_2 partial pressure range from 0–0.8 Pa (Fig. S4(b)). Even the initial rate under oxygen-free conditions was comparable with that obtained at an O_2 pressure of 0.2 Pa. This result shows that the active oxygen species involved in the reaction mainly originated from the oxygen already present on or in the solid, not directly from O_2 gas.

If there is no interaction between the two phases in the catalyst ($VSbO_4$ and α-Sb_2O_4), the activities of $VSbO_4$ and α-Sb_2O_4 domains would not show any size dependence. Fig. 2 shows the formation rate of acrolein from propene oxidation on the precisely designed α-Sb_2O_4/$VSbO_4$/Si catalysts with different separation distances (L025S100, L050S200, L100S400, L400S1600, and L800S3200). A Si substrate and $VSbO_4$/Si were used as reference catalysts. No acrolein was formed on the Si substrate, while $VSbO_4$/Si gave an acrolein formation rate of 1.0×10^{-12} mol·min^{-1}·cm^{-2} at 523 K. Compared with the reference catalysts, the precisely designed α-Sb_2O_4/$VSbO_4$/Si samples showed higher acrolein formation rates ranging from 2 to 7 × 10^{-12} mol·min^{-1}·cm^{-2}. As the separation between ribbons decreased, the acrolein production rate increased. The L100S400 catalyst showed the highest activity of the catalysts of 6.5×10^{-12} mol·min^{-1}·cm^{-2}. The activity of L100S400 was 2.5 times higher than that of L800S3200. Catalyst activities at 473 and 573 K are presented in Fig. S5 and Fig. S6, respectively. The acrolein generation rate increased with temperature on all the catalysts. Table S1 shows the apparent activation energies of the α-Sb_2O_4/$VSbO_4$/Si catalysts calculated for the α-Sb_2O_4/$VSbO_4$/Si samples, which were around 34–163 kJ·mol^{-1}. The apparent activation energy first increased with the width of the α-Sb_2O_4 ribbons (L100S400 possessed the maximum value), and then decreased. We have concluded that there are interaction between two

phases and the interaction depends on the mesoscopic scale through the surface diffusion of material (oxygen atoms) as proposed by Delmon et al. in their remote control mechanisms.[15]

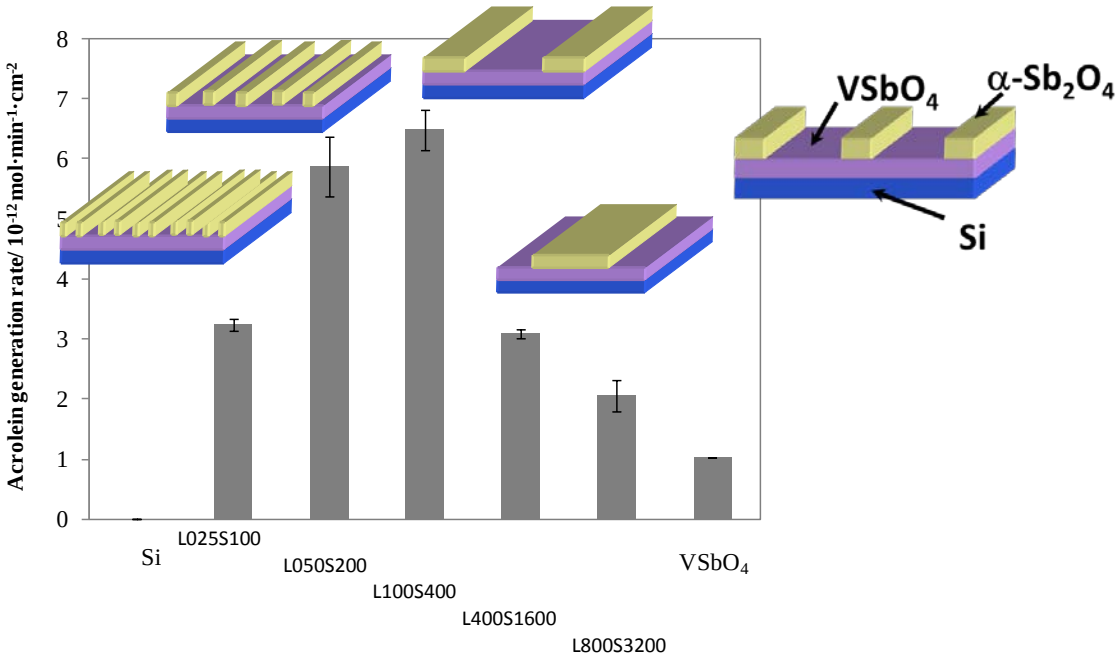

Figure 2 Generation rates of acrolein from propene oxidation (523 K, 0.2 Pa propene, 0.2 Pa O_2, 0.6 Pa Ar) on precisely designed α-Sb_2O_4/$VSbO_4$/Si catalysts with different ribbon separation values but the same ratio of ribbon separation to width of 4:1 (L025S100, L050S200, L100S400, L400S1600, and L800S3200). The generation rates of $VSbO_4$/Si, and a Si substrate were give for reference.

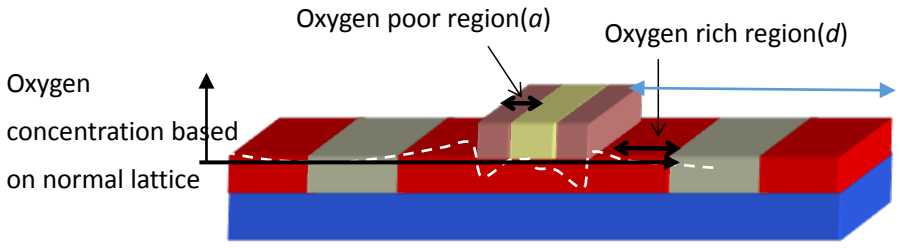

Figure 3 Proposed reaction mechanism based on the surface diffusion model in which separation is larger than the diffusion distance. The white lines represent proposed oxygen concentration.

Now, we discuss a reaction mechanism based on the surface diffusion model which is illustrated in Fig. 3. Both α-Sb_2O_4 and $VSbO_4$ have small amount of oxygen defects. We assume that an oxygen atom on α-Sb_2O_4 has higher chemical potential than that on $VSbO_4$. Oxygen diffusion from α-Sb_2O_4 to $VSbO_4$ occurs in advance before the propene oxidation. Otherwise the initial rates would not show the strong dependence on width/separation ratio observed experimentally. Thus at the investigated reaction temperatures (473–573 K), an oxygen gradient should form, as illustrated by the dashed white line in Fig. 3. The α-Sb_2O_4/$VSbO_4$ thin film contains oxygen-poor and oxygen-rich domains in the α-Sb_2O_4 and $VSbO_4$ regions, respectively. The oxygen-rich domain of $VSbO_4$ is more active toward propene than the normal lattice oxygen on the $VSbO_4$ sites not affected by α-Sb_2O_4. Meanwhile, the oxygen-poor domain in α-Sb_2O_4 has more oxygen defects than the rest of α-Sb_2O_4. These defects will behave as active O_2 dissociation sites and supply active oxygen to the $VSbO_4$ oxygen-rich domain. We assume that the reaction rate (r) is proportional to the sizes of oxygen-rich and oxygen-poor domains,

$$r \propto a * d * N \ , \tag{1}$$

where a and d are the size of oxygen-poor and oxygen-rich domians, respectively, and N is the number of oxygen-rich domains, which can be written as

$$N = \frac{CL}{m+n} = \frac{CL}{5m} \tag{2}$$

where CL is a catalyst side length of the square-shape catalyst. In this case it is 0.6 cm(=6×10^3 μm). Accordingly,

$$r \propto a * d * N = a * d * \frac{CL}{5m} \tag{3}$$

In the case of $2a<m$ and $2d<n$, the reaction rates increase as the ribbon width (m) decreases because the number of active oxygen-rich and -poor domains increases as m decreases according to eq. (3). When $2a>m$ is satisfied, the oxygen-poor region that supplies active oxygen is limited by m.

$$r \propto \frac{m}{2} * d * N = d * \frac{CL}{10} \tag{4}$$

Thus, the dependence of catalyst activity on size will be cancelled out. Furthermore, in the case of $2d>n$, the active oxygen-rich region is limited by n.

$$r \propto \frac{m}{2} * \frac{n}{2} * N = n * \frac{CL}{20} \tag{5}$$

and the activity is proportional to n. Although N(the number of oxygen-rich domains present at the border) were maximum in L025S100, the sizes of the oxygen-rich region and of oxygen-poor or oxygen supply region were both limited by m and n so that it showed lower activity than L100 S400.

It is expected that a and d will vary with temperature because oxygen diffusion requires an activation energy. The oxygen diffusion distance increases with temperature, so the optimal m of the α-Sb_2O_4 ribbons for the maximum acrolein formation rate depends on the temperature, as observed in Fig. 2, S5, and S6. The large activation energies of L050S200–L400S1600 in Table S1 can be explained by the reaction mechanism switching from low activity ($2a<m$, $2d<n$) to higher activity ($2a>m$). In contrast, L025S100 and L800S3200 always maintained the conditions of $2a>m$ and $2a<m$, $2d<n$, respectively, for all temperatures studied here.

In the remote control mechanism, the surface lattice oxygen on $VSbO_4$ plays an important role in catalytic activity. The surface lattice oxygen is consumed during the reaction and the oxygen diffusing from α-Sb_2O_4 replenishes the consumed oxygen on the $VSbO_4$ lattice [15,25]. Conversely, according to our mechanism proposed here, excess oxygen on $VSbO_4$ that has migrated in advance from α-Sb_2O_4 selectively oxidizes propene.

In this work, we demonstrated the feasibility of controlling and tuning the reaction properties of α-Sb_2O_4/$VSbO_4$/Si samples by adjusting the Sb_2O_4 ribbon width and separation on the mesoscopic scale. Lithography is an attractive method to fabricate catalysts with precisely designed mesoscopic structure and it will lead to a new catalyst preparation methods that involve computer-controlled design and manufacture.

The work is supported by the fuel cell project of NEDO(New energy development organization) and Exploratory Research program of Grants-in-Aid for Scientific Research of the Ministry of Education, Culture, Sports, Science and Technology, No 14654127 (2002–2003). We would like to express our thanks to Prof. Bruce C. Gates (UC Davis) for his fruitful discussion. We thank to Dr. Y. Ominami(Hitachi High Tech), Dr. M.Nagase(Tokushima University), Dr. H.Ishii(Toyohashi Technical University), Prof. K.Mukasa(Hokkaido University) and Prof. K.Sueoka(Hokkaido University) for their technical help and discussion to prepare the sample by lithography. The home-made batch reaction system was constructed by the technical stuffs in Institute for Catalysis, Hokkaido University.

[1] A.H. Zewail, J.M. thomas, 4D Electron Microscopy - Imaging in space and time, Imperial College Press, London, 2009.

[2] J. Wolff, A.G. Papathanasiou, H.H. Rotermund, G. Ertl, X. Li, I.G. Kevrekidis, *Phys. Rev. Lett.*, 90 (2003) 018302.

[3] S. Sato, H. Niimi, S. Suzuki, W.J. Chun, K. Irokawa, H. Kuroda, K. Asakura, *Chem. Lett.* 33 (2004) 558.

[4] M.G. Moula, S. Sato, K. Irokawa, H. Niimi, S. Suzuki, K. Asakura, H. Kuroda, *Bull.Chem.Soc.Jpn.*, 81 (2008) 836.

[5] I.Zuburtikudis and H. Saltsburg, *Science* **258**(1992) 1337.

[6] M. D.Graham, I. G. Kevrekidis, K. Asakura, J. Lauterbach, K. Krischer, H.H. Rotermundand G. Ertl, *Science* **264**(1994) 80.

[7] M.X.Yang, D.H.Gracias, P.W. Jacobs, and G.A. Somorjai, *Langmuir* **14** (1998) 1458.

[8] S.Johansson, E.Fridell, and B. Kasemo, *J. Catal.* **200** (2001) 370.

[9] I. Oesterlund., A.W. Grant, B. Kasemo, in: U. Heiz, U. Landman (Eds.), *Nanocatalysis*, Springer, Berlin, 2006, p. 269.

[10] M.Laurin, V.Johanek, A.W.Grant, B. Kasemo, J. Libuda, and H.J. Freund, *J. Chem. Phys.* **122** (2005) 084713.

[11] Y.Ohminami, S. Suzuki, N. Matsudaira, T. Nomura, W.J. Chun, K. Ijima, M. Nakamura, K.Mukasa, M. Nagase, and K. Asakura, *Bull. Chem. Soc. Japan* **78** (2005) 435.

[12] E.Kadossov, S. Cabrini and U. Burghaus, *J. Mol. Catal. A: Chem.* **321** (2010) 101

[13] Y. Moro-Oka, Y. and W. Ueda, *Adv. Catal.* **40** (1994) 233.

[14] I.E.Wachs and K. Routray, *ACS Catal.* **2** (2012) 1235.

[15] B.Delmon and G.F. Froment, *Catal. Rev.* **38** (1996) 69.

[16] E.V.Dehmlow and S.S. Dehmlow, “Phase Transfer Catalysis,” VCH, Weinheim (1993).

[17] L.T.Weng, N.Spitaels, B.Yasse, J. Ladriere, P. Ruiz and B. Delmon, *J. Catal.* **132**(1991) 319.

[18] B.Zhou, E. Sham, T. Machej, P. Bertrand, P. Ruiz and B. Delmon, *J. Catal.* **132**, (1991) 157.

[19] E.M.Gaigneaux, P.Ruizand and B. Delmon, *Catal. Today* **32**(1996) 37..

[20] D.Carson, G.Coudurier, M.Forissier, J.C.Vendrine, A. Laarif and F. Theobald, *J. Chem. Soc., Faraday Trans.* **1**, 79 (1983) 1921.

[21] E.M.Gaigneaux, P. Ruiz, E.E. Wolf and B. Delmon, *Appl. Surf. Sci.* 121(122) (1997) 552.

[22] P.B.Weisz and E.W.Swegler, *J. Phys. Chem.* 59(1955) 823.

[23] P.B.Weisz and E.W.Swegler, *Science* 126 (1957)31.

[24] Y.Haraguchi, T.Wada, Y. Ominami, N. Matsudaira, H. Ariga, S. Takakusagi, K. Asakura, J. *Surf.Sci.Soc. Jpn.*, 33 (2012) 426.

[25]E.M.Gaigneaux, H.M. Abdel Dayem, E. Godard and P.Ruiz, *Appl. Catal. A* **202** (2000) 265